AD-A157 355 A MECHANISM FOR IGNITION OF HIGH-TEMPERATURE GASEOUS NITROMETHANE - THE K.. (U) NAVAL RESEARCH LAB WASHINGTON DC R GUIRGUIS ET AL. 08 JUL 85 NRL-MR-5558 1/1

UNCLASSIFIED F/G 7/3 NL

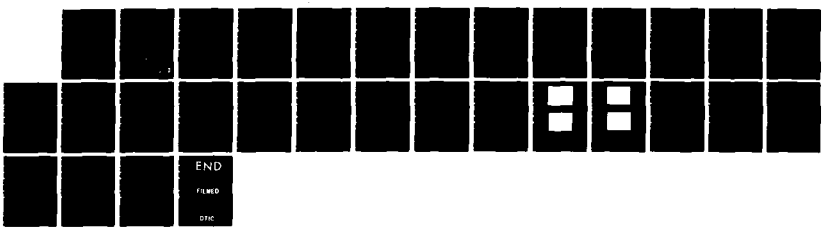

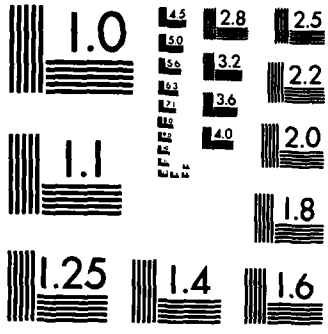

NRL Memorandum Report 5558

A Mechanism for Ignition of High-Temperature Gaseous Nitromethane — The Key Role of the Nitro Group in Chemical Explosives

R. GUIRGUIS,* D. HSU,† D. BOGAN† AND E. ORAN

Laboratory for Computational Physics

**Berkeley Research Associates*
Springfield, VA 22150

†*Combustion and Fuels Branch*
Chemistry Division

July 8, 1985

This research was supported by the Office of Naval Research.

NAVAL RESEARCH LABORATORY
Washington, D.C.

AD A157 355

SECURITY CLASSIFICATION OF THIS PAGE

REPORT DOCUMENTATION PAGE

1a REPORT SECURITY CLASSIFICATION UNCLASSIFIED	1b. RESTRICTIVE MARKINGS
2a SECURITY CLASSIFICATION AUTHORITY	3 DISTRIBUTION / AVAILABILITY OF REPORT
2b DECLASSIFICATION / DOWNGRADING SCHEDULE	Approved for public release; distribution unlimited.
4 PERFORMING ORGANIZATION REPORT NUMBER(S) NRL Memorandum Report 5558	5. MONITORING ORGANIZATION REPORT NUMBER(S)
6a NAME OF PERFORMING ORGANIZATION Naval Research Laboratory 6b OFFICE SYMBOL (If applicable) Code 4040	7a. NAME OF MONITORING ORGANIZATION
6c ADDRESS (City, State, and ZIP Code) Washington, DC 20375-5000	7b. ADDRESS (City, State, and ZIP Code)
8a. NAME OF FUNDING / SPONSORING ORGANIZATION Office of Naval Research 8b. OFFICE SYMBOL (If applicable)	9. PROCUREMENT INSTRUMENT IDENTIFICATION NUMBER
8c. ADDRESS (City, State, and ZIP Code) Arlington, VA 22217	10 SOURCE OF FUNDING NUMBERS PROGRAM ELEMENT NO: 61153N-13 PROJECT NO: RR013-06-4F TASK NO: WORK UNIT ACCESSION NO: 44-0313-A-5

11 TITLE (Include Security Classification) A Mechanism for Ignition of High-Temperature Gaseous Nitromethane — The Key Role of the Nitro Group in Chemical Explosives

12 PERSONAL AUTHOR(S)
Guirguis, R.,* Hsu, D., Bogan, D. and Oran, E.

13a TYPE OF REPORT	13b TIME COVERED	14 DATE OF REPORT (Year, Month, Day)	15. PAGE COUNT
Interim	FROM ____ TO ____	1985 July 8	30

16 SUPPLEMENTARY NOTATION *Berkeley Research Associates, Springfield, VA 22150

This research was supported by the Office of Naval Research.

17 COSATI CODES			18 SUBJECT TERMS (Continue on reverse if necessary and identify by block number)
FIELD	GROUP	SUB-GROUP	Nitromethane, Explosives, Chemical kinetics, Shock tube

19 ABSTRACT (Continue on reverse if necessary and identify by block number)

A detailed chemical mechanism describing ignition of high-temperature pure gaseous nitromethane was compiled and tested using shock tube experiments. The temperatures and pressures behind the reflected shock were in the range 1000 to 1600 K and 1 to 10 atm. Measurements were made of the time evolution of the pressure at the end wall, as well as of the simultaneous pressure and NO absorption a short, fixed distance from the end wall. Mass and infrared spectroscopy were used to identify the final products. In the reaction mechanism proposed, initiation starts with the C-N bond breaking which yields CH_3 and NO_2. Methoxy and CH_2NO_2 radicals then propagate the reaction through two major parallel pathways, both producing CH_2O. Formaldehyde is then reduced to HCO and carries the reaction towards completion. The radical reactions do not release enough energy to compensate for the energy consumed in breaking the C-N bond. Although most of the radicals reach their maximum concentration early in the reaction process, ignition does not occur until virtually all of the

(Continues)

20 DISTRIBUTION / AVAILABILITY OF ABSTRACT	21 ABSTRACT SECURITY CLASSIFICATION
☒ UNCLASSIFIED/UNLIMITED ☐ SAME AS RPT ☐ DTIC USERS	UNCLASSIFIED
22a NAME OF RESPONSIBLE INDIVIDUAL E. Oran	22b TELEPHONE (Include Area Code) (202) 767-2960 22c. OFFICE SYMBOL Code 4040

DD FORM 1473, 84 MAR 83 APR edition may be used until exhausted
All other editions are obsolete

SECURITY CLASSIFICATION OF THIS PAGE

19. ABSTRACT (Continued)

nitromethane is consumed. The calculations show that the nitro group is the key to explosion: NO_2 produces OH through its reaction with H radicals. Hydroxyl reactions, which are fast and exothermic, lead to an accelerated consumption of the explosive with heat release. Comparison with the experiments shows that the mechanism predicts correct induction times for the pressure and temperature range of the experiments.

CONTENTS

A MECHANISM FOR IGNITION OF HIGH-TEMPERATURE GASEOUS NITROMETHANE — THE KEY ROLE OF THE NITRO GROUP IN CHEMICAL EXPLOSIVES

INTRODUCTION

The first studies of nitromethane pyrolysis were reported by Taylor and Vesselovsky [1] and Hirschlaff and Norrish [2]. Considerably later, plausible initiation steps were deduced by Cottrell, Graham and Reid [3] and Hillenbrand and Kilpatrick [4]. The first accurate measurement of the rate of unimolecular decomposition of nitromethane and the effects of pressure was done by Glänzer and Troe [5] using a shock tube. This work established that C-N bond rupture is the only plausible initial step. Most recently, Perche, Tricot and Lucquin [6] made the first attempt to construct a detailed chemical kinetic mechanism for the decomposition of nitromethane. Their scheme was applied to the low-temperature decomposition of nitromethane vapor at very low pressures.

The present study presents a chemical reaction mechanism that describes the ignition of pure gaseous nitromethane at high temperatures and identifies the key role of the NO_2 group in promoting ignition. This work was undertaken as a first step in understanding the chemistry of pure solid explosives. The elementary reaction rate constants pertinent to the decomposition of nitromethane have either been collected from the literature or estimated. No attempt was made to measure any new rate constant or to confirm a previously measured one. Instead, the predictions of the compiled kinetic mechanism were tested by comparing them with measured induction times. Mass and infrared spectroscopy were used to identify the final products. Most of the experiments

Manuscript approved January 28, 1985.

used pure nitromethane vapor, although some used mixtures of nitromethane diluted in argon to obtain higher temperatures at relatively low pressures. Temperatures and pressures behind the reflected shock were in the range 1000 to 1600 K and 1 to 10 atm.

Traditionally, shock tube experiments with 100% concentration have been avoided because of the large departure of the gasdynamic configuration from one-dimensionality. In such cases, calculating the rate of decomposition requires complicated corrections to the effective heating time and temperature. However, since the experiments performed here measured the induction time only, the pressure at the center of the end plate is an adequate diagnostic provided that proper care is taken to measure the incident shock velocity and to evaluate the temperature behind the reflected shock. The details of the experimental arrangement and diagnostics are given below. The inherently one-dimensional flow character at the center of the end plate [7] combined with a very short induction time, as is the case with nitromethane at high temperatures, allowed the use of a one-dimensional calculation to evaluate the conditions behind the reflected shock.

The role of the nitro group, NO_2, in causing rapid-exothermic ignition was tested by deleting $NO_2 + H \longrightarrow OH + NO$ from the set of reactions describing the decomposition process. Calculated induction times and final temperatures were then compared to those calculated using the full set of reaction kinetics. In all cases, the induction time was very sensitive to the above reaction rate. Below we describe the experiment, and discuss the chemical kinetic mechanism and the key role of the nitro group in chemical explosives.

EXPERIMENT

A 6.35 cm internal diameter shock tube was used which had a 2.52 m driver section and a 3.8 m shock section. Helium was pumped in the driver section until the diaphragm burst, so that shocks of various Mach numbers were achieved by changing the diaphragm thickness. Four piezoelectric gauges located near the end plate detected the instant of shock arrival and allowed us to evaluate the incident shock velocity free of the error which may result from its attenuation. A CO laser probe and a quartz pressure gauge measured the NO absorption and the pressure evolution at a fixed location 4.5 cm from the end wall. A second pressure gauge measured the pressure evolution at the end wall.

After all of the wave effects in the shock tube died out and mixing was complete, samples of the products were extracted for later analysis by mass spectrometry. The contents of the shock tube were then pumped through a liquid nitrogen trap. After warming up the contents to room temperature, an infrared spectrometer was used to identify the condensible products. The analysis of collected products was used to confirm the significant species formed in the decomposition process. No attempt was made to measure species concentrations in the final products. Since absorption profiles depend on temperature, the measured real-time NO absorption gave only qualitative evidence of the NO behavior.

Generally, the unshocked gas consisted of 100% spectro-grade nitromethane at pressures up to a few torr. In a few cases, argon was mixed with nitromethane so that the mixture could be shocked to high temperatures without increasing the driver pressure excessively and therefore avoiding damage to the piezoelectric and quartz pressure gauges. However, the dilution causes ignition to be less pronounced on the pressure trace and consequently more difficult to detect.

The conditions behind the reflected shock were calculated from the observed incident shock velocity assuming frozen composition across the shock waves and equilibrium of the internal modes of the nitromethane molecules. The effect of the variation of the heat capacity with temperature was included. The recorded pressure jumps at the end wall were found to compare favorably with those calculated. Temperatures and pressures in the range 1000 - 1600 K and 1 - 10 atm were achieved. The reflected shock moves into a narrowing channel due to the boundary layer formed behind the incident shock. Unlike the idealized one-dimensional problem, in this case the gas behind the reflected shock does not come to zero velocity. Instead, a small residual motion slowly compresses the gases at the wall. Because of the very short induction times of nitromethane, the effect of this compression process is ignored and a constant volume adiabatic process starting at the calculated temperature and pressure behind the reflected shock is assumed for the numerical simulation. However, for low-temperature shocks, when the heating due to the subsequent slow compression is comparable to the sudden heating upon crossing the shock, the induction time for an adiabatic process starting immediately after the reflected shock can be significantly longer than the measured one.

REACTION MECHANISM

The elementary reactions describing the decomposition of nitromethane at high temperatures are given in Table I. These are either obtained from the literature or estimated. Numerical integration [34] of the rate equations given in Table I gives the chemical species evolution as a function of time. Tabulated or estimated enthalpies and heat capacities [22a,32] of the chemical species were used to calculate the temperature as a function of time. Gas-dynamics effects were not calculated. Instead, an adiabatic constant volume process is assumed.

The initiation step is that deduced by Glanzer and Troe [5] for low pressures,

$$CH_3NO_2 + M \longrightarrow CH_3 + NO_2 + M.$$

The major overall pathways can be inferred from the computations. These show that the reaction proceeds mainly by two parallel pathways, as shown in Fig. (1). The first involves H abstraction from nitromethane by radicals to form CH_2NO_2, which unimolecularly decomposes into formaldehyde. The second pathway starts with the methyl plus nitrogen dioxide reaction to form methoxy radicals, which decompose almost instantaneously into formaldehyde. The formaldehyde from both pathways is then attacked by radicals to produce formyl radicals, which decompose or react with NO_2 to produce CO. A third minor pathway (not shown in Fig. (1)) involves the two carbon (C_2) species, whose reactions are included in Table I.

The proposed reaction scheme is not intended to be all inclusive. Only those reactions (and reverse reactions) having rates within three orders of magnitude of the fastest rates and those leading to observed products were retained in Table I.

TABLE - I -

Reaction Rate Constants, $k = A\ T^n e^{-E/RT}$

Reactants	Products	A	n	E	Ref.
Initiation					
$CH_3NO_2 + M$	$CH_3 + NO_2 + M$	1.30(17)	0.00	42.000	5
Basic Reactions					
$CH_3 + NO_2$	$CH_3O + NO$	1.30(13)	0.00	0.000	5
CH_3O (M)	$CH_2O + H$ (M)[a]	3.31(15)	0.00	27.500	
	$k_p = k \times 0.10615\ (\ [M]\ T\ )^{0.65}$				12
$NO_2 + H$	$NO + OH$	3.50(14)	0.00	1.500	10
$CH_3O + OH$	$CH_2O + H_2O$	3.20(13)	0.00	0.000	8
$H_2 + OH$	$H_2O + H$	2.20(13)	0.00	5.150	15
$H_2O + H$	$H_2 + OH$	9.30(13)	0.00	20.400	15
$CH_3O + NO_2$	$CH_2O + HONO$	4.00(11)	0.00	0.000	9
$CH_3O + NO$	$CH_2O + HNO$	3.2(12)	0.00	0.000	9
$HONO + M$	$NO + OH + M$	3.00(18)	0.00	46.700	9
$NO + OH + M$	$HONO + M$	7.91(15)	0.00	-2.200	b
$HNO + M$	$NO + H + M$	2.88(16)	0.00	48.800	10
$NO + H + M$	$HNO + M$	5.40(15)	0.00	-0.600	10
$CH_3NO_2 + CH_3$	$CH_2NO_2 + CH_4$	1.60(11)	0.00	10.800	23
$CH_3NO_2 + H$	$CH_2NO_2 + H_2$	6.30(13)	0.00	9.700	30
$CH_3NO_2 + OH$	$CH_2NO_2 + H_2O$	1.85(12)	0.00	1.635	17
CH_2NO_2 (M)	$CH_2O + NO$ (M)[a]	1.00(13)	0.00	36.000	6
Formyl production					
$CH_2O + CH_3$	$HCO + CH_4$	3.10(10)	0.00	4.860	31
$CH_2O + H$	$HCO + H_2$	1.26(13)	0.00	3.760	25
$CH_2O + OH$	$HCO + H_2O$	7.53(12)	0.00	0.175	20

(continued on next page)

TABLE - I - (continued)

Reactants	Products	A	n	E	Ref.
Products formation					
HCO + M	CO + H + M	1.00(15)	0.00	14.700	11
CO + H + M	HCO + M	6.90(14)	0.00	-1.700	16
HCO + NO_2	HONO + CO	1.00(14)	0.00	0.000	9
HCO + NO	HNO + CO	2.00(11)	0.50	2.000	8
HCO + HNO	CH_2O + NO	3.20(13)	0.00	1.360	8
CO + OH	CO_2 + H	$\log_{10}k = 10.83 + 3.94(-4) \times T$			16
CH_4 + OH	CH_3 + H_2O	1.45(12)	0.00	3.400	19
Two-Carbons Group Reactions					
CH_3 + CH_3 (M)	C_2H_6 (M)[a]	3.16(13)	0.00	0.000	27
C_2H_6 + CH_3	C_2H_5 + CH_4	3.20(11)	0.00	10.800	22
C_2H_6 + H	C_2H_5 + H_2	1.26(14)	0.00	9.700	29
C_2H_6 + OH	C_2H_5 + H_2O	1.10(13)	0.00	2.440	17
C_2H_5 + H (M)	CH_3 + CH_3 (M)[a]	3.71(13)	0.00	0.000	26
C_2H_5 + M	C_2H_4 + H + M	4.70(14)	0.00	26.600	11
C_2H_4 + OH	CH_2O + CH_3	4.50(12)	0.00	0.200	21
C_2H_4 + OH	C_2H_3 + H_2O	7.33(12)	0.00	7.800	17
C_2H_3 + M	C_2H_2 + H + M	8.00(14)	0.00	31.500	13
Methanol Group Reactions					
CH_3 + OH (M)	CH_3OH (M)[a]	8.00(12)	0.00	0.000	11
CH_3OH + CH_3	CH_2OH + CH_4	3.15(10)	0.00	6.360	31
CH_3OH + H	CH_2OH + H_2	1.50(13)	0.00	5.260	24
CH_3OH + OH	CH_2OH + H_2O	4.23(12)	0.00	0.850	18
CH_2OH (M)	CH_3O (M)[a]	1.00(13)	0.00	39.500	28
CH_2OH + H	CH_2O + H_2	7.50(13)	0.00	0.000	24

(continued on next page)

TABLE - I - (continued)

Reactants	Products	A	n	E	Ref.
Nitrosomethane Group Reactions					
CH_3 + NO (M)	CH_3NO (M)[a]	4.00(12)	0.00	0.000	6
CH_3NO (M)	CH_3 + NO (M)[a]	7.00(13)	0.00	38.000	6
CH_3NO + CH_3	CH_2NO + CH_4	1.60(11)	0.00	10.800	23
CH_3NO + H	CH_2NO + H_2	6.30(13)	0.00	9.700	30
CH_3NO + CH	CH_2NO + H_2O	1.85(12)	0.00	1.635	17
CH_2NO (M)	HCN + OH (M)[a]	3.98(11)	0.00	33.000	14

(a) Rate constants of reactions with '(M)' have a pressure fall-off curve. Units of rate constant are indicated by number of reactant species, where the parenthetical (M) does not count. For example, the rate constant for CH_3NO_2 + M has units cm^3/mol s, that for CH_3O (M) has units s^{-1}, and that for NO + OH + M has units cm^6/mol^2 s. Activation energy is given in Kcal/mol.

(b) Reverse reaction rate evaluated from preceeding forward reaction rate and equilibrium thermochemistry.

REFERENCES

1. Taylor, H. and Vesselovsky, V., J. Phys. Chem. 39, 1095 (1935).
2. Hirsclaff, E. and Norrish, R., J. Chem. Soc., 1580 (1936).
3. Cottrell, T., Graham, T., and Reid, T., Trans. Far. Soc. 47, 584 (1951).
4. (a) Hillenbrand, L. and Kilpatrick, M., J. Chem. Phys., 19, 381 (1951).
   (b) Hillenbrand, L. and Kilpatrick, M., J. Chem. Phys., 21, 525, (1951).
5. Glanzer, K. and Troe, J., Helv. Chim. Acta, 55, 2884 (1972).
6. Perche, A., Tricot, J., and Lucquin, M., J. Chem. Res. (S) 304, (M) 3219 (1979).
7. Belford, R. and Strehlow, R., Ann. Rev. Phys. Chem., 20, 247 (1969).
8. Westley, F., Table of Recommended Rate Constants for Reactions Occuring in Combustion, NSRDS-NBS-67, U.S. Dept. Commerce, 1980.
9. Fifer, R., Seventeenth Symp. (Int.) on Combustion, p. 587, The Combustion Institute, Pittsburgh, 1978.
10. Baulch, D., Drysdale, D., and Horne, D., Evaluated Kinetic Data for High Temperature Reactions, Vol. 2, The University of Leeds, 1972.
11. Hsu, D., Shaub, W., Creamer, T., Gutman, D., and Lin, M., Ber. Bunsenges. Phys. Chem. 87, 909 (1983).
12. (a) Adams, G.F., Chemical and Physical Processes in Combustion, Proceedings of the 1978 Eastern States Section of the Combustion Institute, The Combustion Institute, Pittsburgh, 1978.
    (b) Adams, G. F., private communication, 1984; increasing the activation from 24.0 to 27.5 kcal/mole was recommended.
13. Benson, S. W. and Haugen, G. R., J. Phys. Chem., 71, 1735 (1967).
14. Golden, D. M., Chemical Kinetic Data Needs for Modeling the Lower Troposhpere, Herron, J.T., Huie, R. E., and Hodgeson, J. A., (eds.) NBS-SP-557, p. 57, U. S. Dept. Commerce, 1979. This reference describes

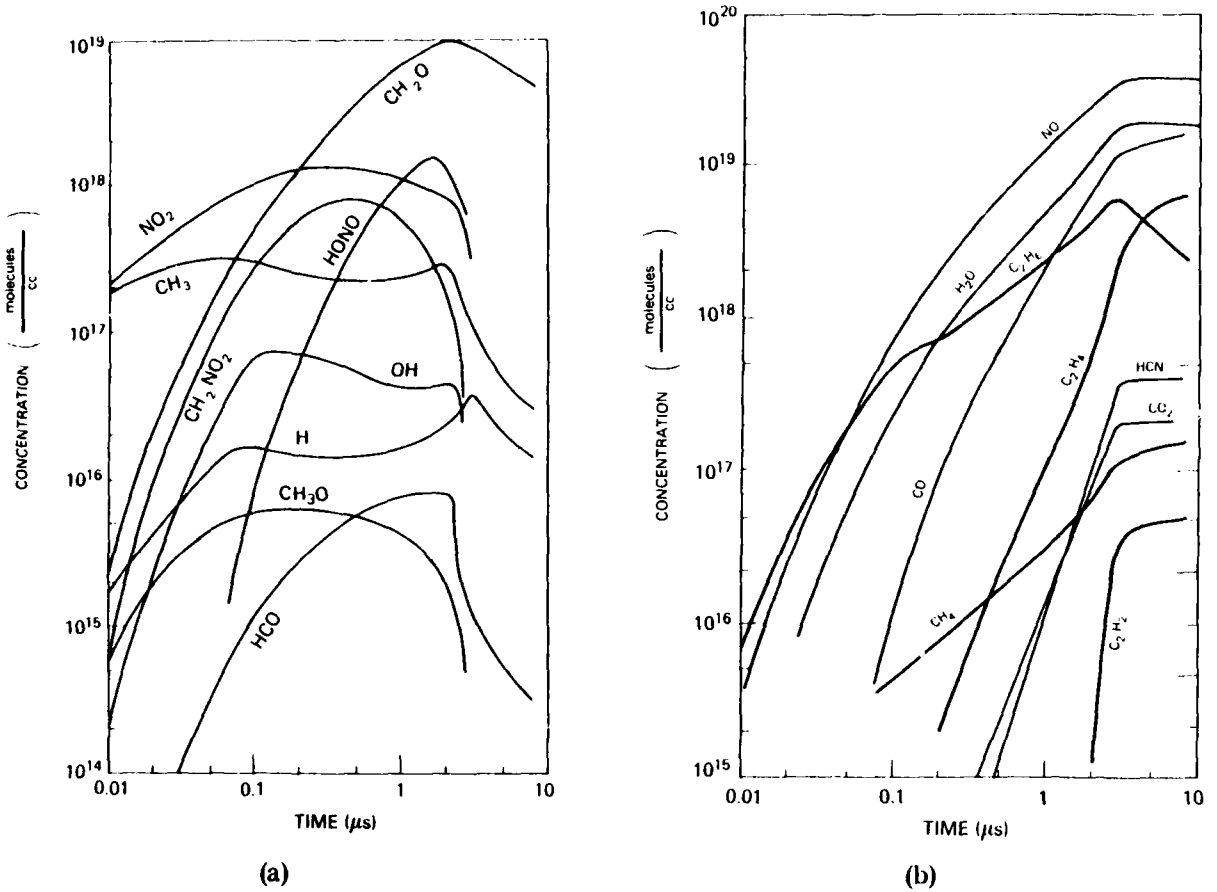

Fig. 4 — Calculated time evolution of (a) intermediate species and (b) stable products concentration of constant volume adiabatic decomposition of 100% nitromethane, starting at 1263 K and 6.96 atm.

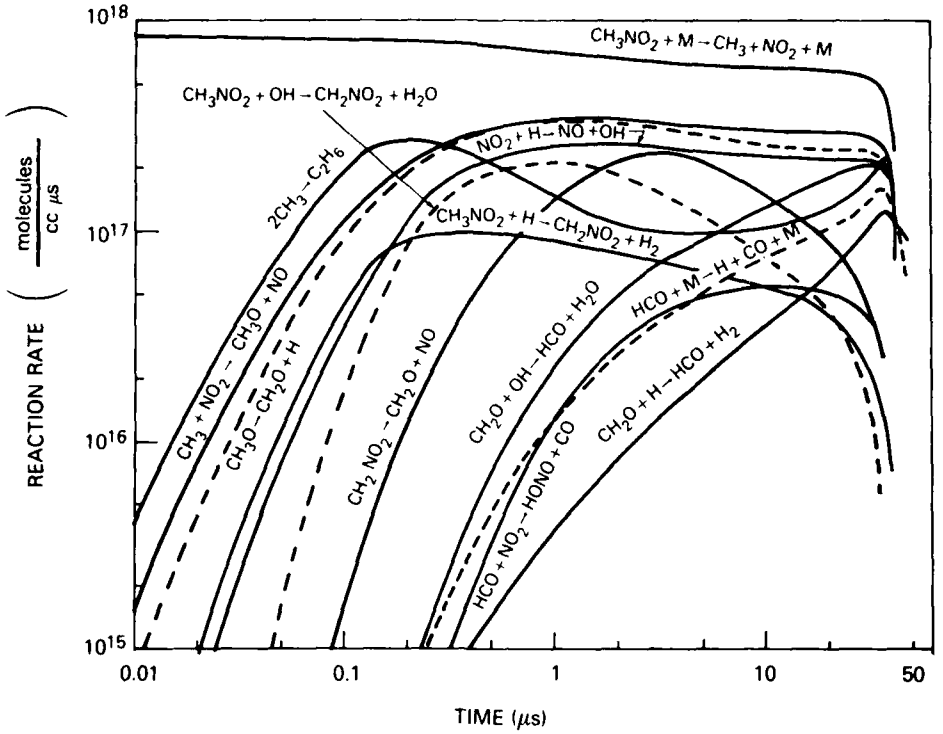

(a)

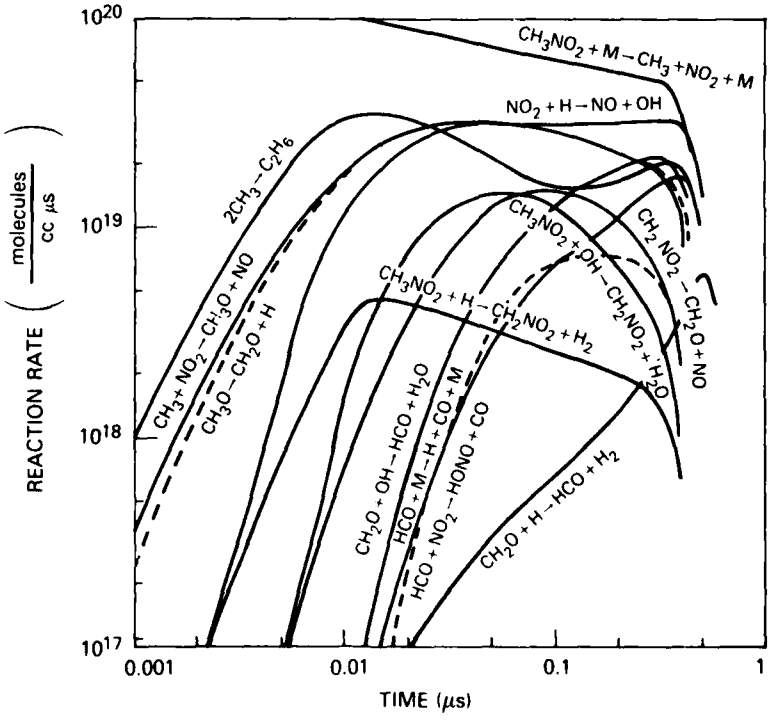

(b)

Fig. 3 — Most significant reaction rates in the decomposition of 100% nitromethane, calculated for an adiabatic constant volume process (a) starting at 1108 K and 3.92 atm, and (b) starting at 1494 K and 5.73 atm.

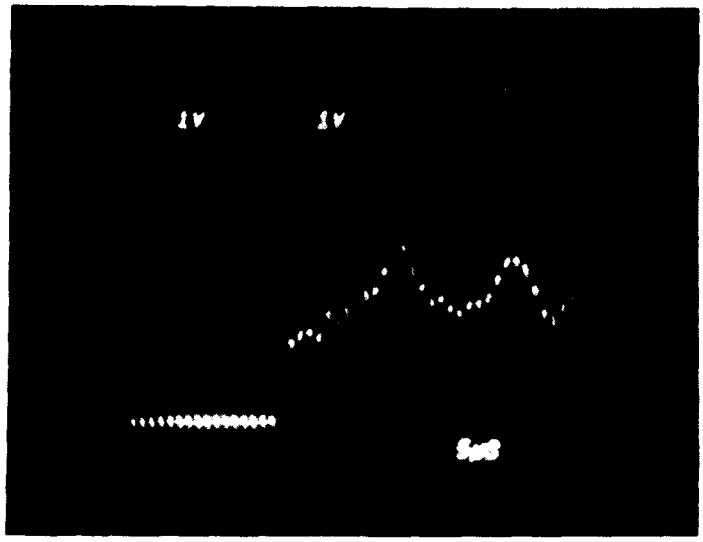

(c) Pressure trace at end wall; 7.7 torr 100% nitromethane; incident shock velocity: 0.122 cm/μs; calculated temperature and pressure behind reflected shock: 1227 K and 4.82 atm; measured induction time: 10-12 μs.

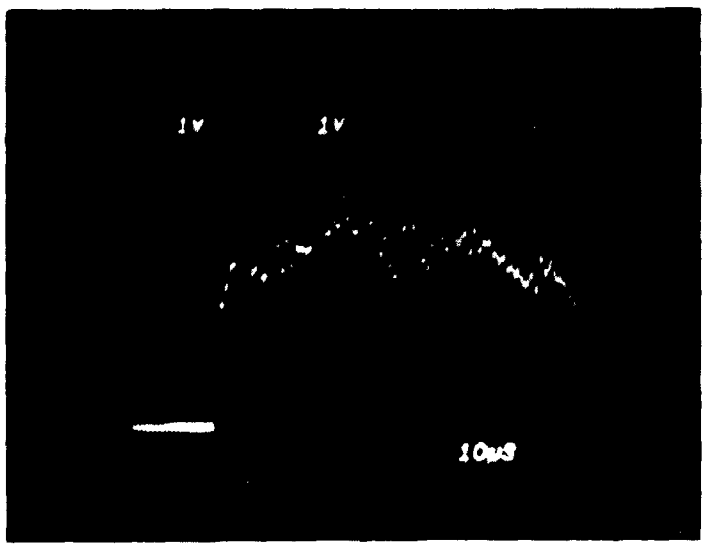

(d) Pressure trace at end wall; 10.31 torr 100% nitromethane; incident shock velocity: 0.125 cm/μs; calculated temperature and pressure behind reflected shock: 1263 K and 6.96 atm; measured induction time: 5 μs.

Fig. 2 (Cont'd) — Pressure and NO absorption traces from the shock tube experiment. Measurements taken either at, or 4.5 cm from, the end wall. Numbers at the top refer to oscilloscope gain per division for pressure and NO traces, respectively. Third number is the time increment per division. Observed oscillations in pressure occuring after the first spike, denoting ignition, should not affect induction time increments.

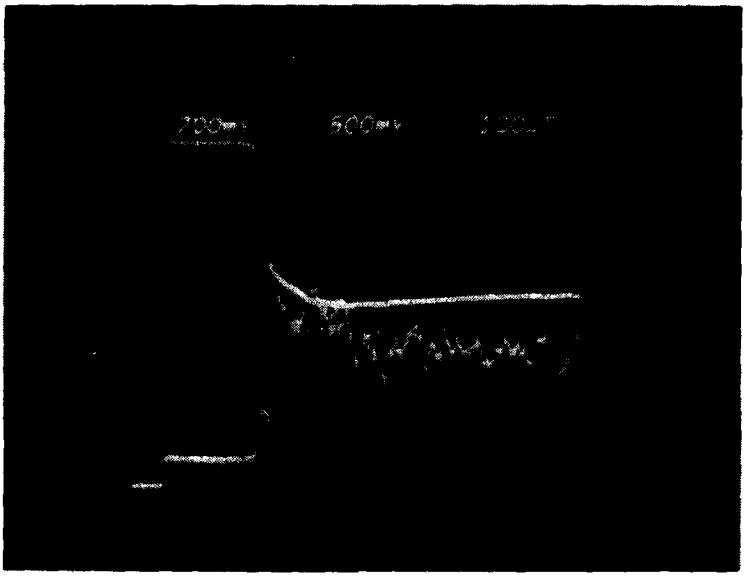

(a) Pressure (lower) and NO (upper) traces 4.5 cm from end wall; mixture: 5.0 torr nitromethane, 14.5 torr argon; incident shock velocity: 0.086 cm/μs; calculated temperature and pressure behind reflected shock: 1145 K and 1.69 atm; measured induction time: 70-80 μs.

(b) Pressure (lower) trace at end wall; NO (upper) trace 4.5 cm from end wall; 18.19 torr 100% nitromethane; incident shock velocity: 0.112 cm/μs; calculated temperature and pressure behind reflected shock: 1108 K and 8.8 atm; measured induction time: 25-30 μs.

Fig. 2 — Pressure and NO absorption traces from the shock tube experiments. Measurements taken either at, or 4.5 cm from, the end wall. Numbers at the top refer to oscilloscope gain per division for pressure and NO traces, respectively. Third number is the time increment per division. Observed oscillations in pressure occuring after the first spike, denoting ignition, should not affect induction time measurements.

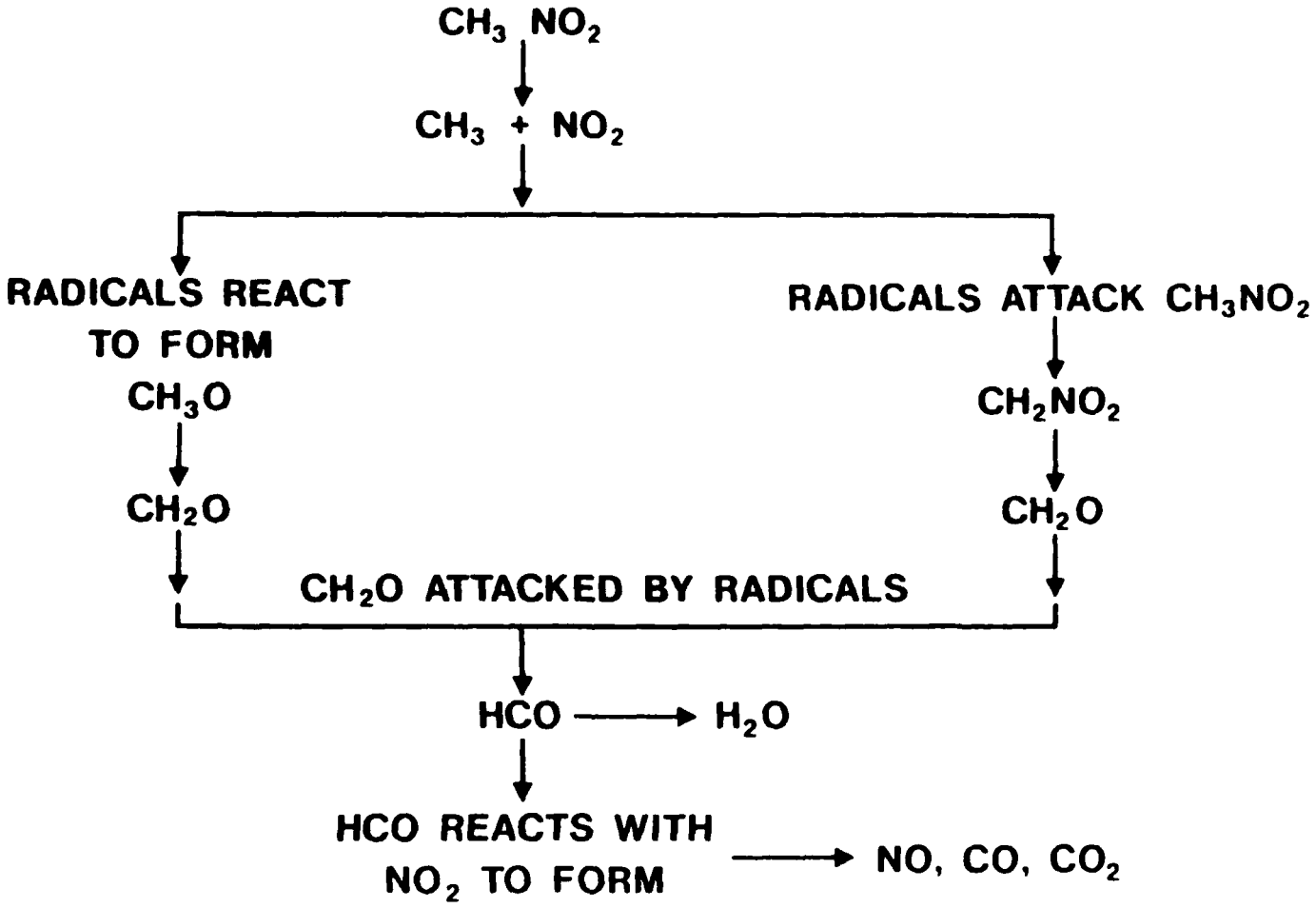

Fig. 1 — Major pathways for the decomposition of gaseous nitromethane

CONCLUSION

The decomposition of CH_3NO_2 proceeds by two major parallel pathways, through methoxy radicals and through CH_2NO_2 radicals. Both pathways produce CH_2O which, when attacked by OH and H radicals, yield HCO radicals that carry the reaction towards completion. As long as unreacted nitromethane remains, its unimolecular (C-N bond rupture) reaction serves as an energy sink, preventing ignition. As a result, although the radical concentrations reach their maximum level early in the overall process, ignition does not occur until all nitromethane is consumed. The energy released then by the radical reactions causes rapid ignition.

The computations show that the reaction

$$NO_2 + H \longrightarrow OH + NO$$

plays a key role in accelerating ignition in nitromethane because it controls the OH concentration, due to the absence of other efficient routes to OH. This effect is expected in other explosives containing C, H and the nitro or nitrate [9] groups, to the extent that other efficient OH formation routes are lacking.

We have compared the predictions of the chemical kinetic scheme to the shock tube experiments. The mechanism proposed gives the correct induction times in the pressure and temperature ranges considered.

ACKNOWLEDGMENTS

This research has been supported by the Office of Naval Research through the Naval Research Laboratory.

TABLE - III -

Calculated Effect of k($H + NO_2 \rightarrow OH + NO$) on Induction Time

Table II Data Point #	Fractional Value of k used[a]	Initial Pressure (Atm)	Initial Temperature (K)	Calculated Induction Time (μs)	Final Calculated Temperature and Time (K, μs)
4	1.0	3.92	1108	35-40	1326, 50
	0.2	3.92	1108	b	1056, 60
	0.0	3.92	1108	b	921, 200
14	1.0	6.96	1263	2-3	1578, 8
	0.2	6.96	1263	4-5	1389, 8
	0.0	6.96	1263	b	1087, 20
17	1.0	5.73	1494	0.4	1839, 1.0
	0.2	5.73	1494	0.5	1727, 4.0
	0.0	5.73	1494	1.2	1429, 30

a The "normal" value of k is that given in Table I and is denoted by an entry of 1.0.

b An entry of b means that ignition did not occur.

The H atom concentration was approximately doubled by setting the rate of $H + NO_2 \longrightarrow OH + NO$ equal to zero. The resulting increase in the rates of the remaining H atom reactions did not shorten the calculated ignition time. This fact, together with the rates plotted in Figs. (3a) and (3b), shows that OH is the key species consuming nitromethane in the radical chain mechanism. It is also interesting to note that the heat released by methyl radical recombination did not promote ignition, unless the radical chain mechanism initiated by $H + NO_2 \longrightarrow OH + NO$ was included.

The effect of varying other selected rate constants was also tested, however systematic sensitivity analyses were not done. In general, the reactions with the largest rates will control the decomposition process, and these are shown in Figs. (3a) and (3b). These reactions have well established, measured rate constants, with a few exceptions. The estimated Arrhenius parameters of Perche et. al. for unimolecular decomposition of CH_2NO_2 [6] could give a rate that is in error by a factor as large as ten. Nevertheless, the lifetime of this radical is short with respect to unimolecular decay, and this decay path is the dominant one for its consumption. We have made estimates, which should be correct to within a factor of three, for the rate constants of the hydrogen abstraction reactions of H and OH with nitromethane [17,30]. Confidence in these estimates is based upon agreement between predicted and measured rate constants for H and OH abstracting hydrogen from C-H bonds in other molecules [17,19,22]. Finally, methyl radical recombination to form ethane, and methoxy radical unimolecular decomposition, have pressure dependent rate constants. Appropriate pressure adjusted values have been used [12,33].

ROLE OF NITRO GROUP

The sensitivity of the calculated induction time to the reaction,

$$NO_2 + H \longrightarrow OH + NO$$

was tested by deleting it from the set of reactions describing nitromethane decomposition. The results, for a representative subset of the initial conditions, are given in Table III. Deleting this reaction drastically increased the induction time at lower temperatures, the difference becoming smaller as the temperature increased. For example, while nitromethane ignites in 35 - 40 μs at 1108 K and 3.92 atm, no sign of ignition was observed after 200 μs when the above reaction was deleted. At 1263 K and 6.96 atm, ignition had not occured after 20 μs compared to 2 -3 μs for the full set of reactions. The induction time only triples from 0.4 to 1.2 μs at 1494 K and 5.73 atm. However, although ignition occured, the overall reaction system remained globally endothermic. The final calculated temperature, 1430 K, is less than the starting temperature, 1494 K, and much smaller than the final temperature calculated with the full set of reactions, 1840 K.

The rapid ignition of nitromethane is attributed to the abundance of NO_2 formed early in the decomposition process, specifically to the rapid reaction of NO_2 with H radicals producing large quantities of OH. The subsequent chain-carrying, H-abstraction reactions of OH with nitromethane and formaldehyde are fast and exothermic and contribute to the release of energy. The reaction of OH with nitromethane accelerates the consumption of starting material, nitromethane. The formaldehyde reaction with OH leads to the regeneration of H which restarts the chain.

TABLE - II -

Calculated and Observed Induction Times

Data Point	% CH_3NO_2	Pressure (atm)	Temperature (K)	Induction Time (μs) Calculated	Measured
<u>100% Nitromethane</u>					
1	100%	4.00	1017	>240[a]	no ignition[b]
2		4.00	1035	>150[a]	no ignition[b]
3		5.78	1030	>150[a]	80
4		3.92	1108	35-40	35-40
5		4.00	1120	30-35	35
6		5.20	1142	15-20	20 and 30-35[c]
7		4.96	1120	25-30	30
8		3.76	1155	15-20	25-30
9		8.80	1108	20-25	25-30
10		7.25	1131	15-20	12 and 25[c]
11		8.17	1180	5-10	7
12		4.82	1227	5-6	10-12
13		6.85	1202	6	10-12
14		6.96	1263	2-3	5
15		6.56	1283	2.2	4
16		6.17	1376	0.8-1	2-3
17		5.73	1494	0.4	< 1[d]
<u>Mixtures of Nitromethane and Argon</u>					
1	26	1.69	1145	60-70	70-80
2	64	3.94	1341	2-3	3-5
3	49	2.18	1440	2-3	4
4	42	4.52	1542	0.5-1	1-2

a Temperature increased slowly. No sudden rise in temperature was observed up to listed time.
b No ignition spike was observed on pressure trace.
c Two ignition spikes were observed on pressure trace. The second was higher in amplitude and sharper.
d Ignition spike undetectable from reflected shock jump on the oscilloscope pressure trace.

Although most of the radicals reach their maximum concentration early in the reaction process, ignition does not occur until all of the nitromethane is consumed. As long as nitromethane is still present, the overall reaction system stays endothermic because the radical reactions do not release enough energy to compensate for the energy consumed in breaking the C-N bond. When the nitromethane is depleted, the system suddenly becomes exothermic and ignition occurs. In this mechanism, all reaction rates drop sharply at ignition without the preceding sudden increase observed in most systems. This behavior is due to the sudden decrease in the concentrations of reactive species which have rapidly reacted to form stable products, without any nitromethane present to replenish them.

Figure (4a) shows the calculated time evolution of the intermediate species for the same initial conditions as in Fig. (2d). The methoxy and hydrogen radicals, which are consumed almost as fast as they are formed, have a very low, nearly steady-state concentration. We note an abundance of NO_2, which, as explained below, accelerates the ignition process. Formaldehyde has the highest concentration of any intermediate, and its depletion begins late in the induction period. Figure (4b) shows the concentrations of stable products steadily increasing until the end of the induction time, 2.5 μs, when they level off. In our calculations, this time coincides consistently with that of consumption of all the nitromethane. We note the same behavior of the NO absorption trace in Fig. (2a).

shock and the ignition spike on the oscilloscope pressure trace. By fitting the calculated induction times for 100% nitromethane to an Arrhenius form we obtain

$$\tau_i = A_i \exp(E_i/RT)$$

where

$$A_i = 6.13 \times 10^{-7}\ \mu s$$

$$E_i = 38.6\ \text{Kcal/mol.}$$

For temperatures above 1600 K the calculations should follow this same expression. We believe that the proposed mechanism should correctly predict ignition behavior up to 2000 K.

The calculated rates of the most significant reactions for the initial conditions, 1108 K, 3.92 atm and 1494 K, 5.73 atm, corresponding to points 4 and 17 in Table II, are shown in Figs. (3a) and (3b), respectively. The same sequence of events is observed in the computations at both temperatures:

* C-N bond in CH_3NO_2 breaks giving $CH_3 + NO_2$
* CH_3 radicals recombine producing C_2H_6
* CH_3 recombines with NO_2 producing CH_3O, which immediately decomposes giving H radicals + CH_2O, and NO
* H radicals attack CH_3NO_2 producing CH_2NO_2 radicals
* H radicals react with NO_2 producing OH radicals and NO
* OH radicals attack CH_3NO_2 producing CH_2NO_2 radicals
* CH_2NO_2 radicals unimolecularly decompose giving more CH_2O
* OH (and H) radicals attack CH_2O giving HCO
* HCO radicals decompose or react with NO_2 to give CO.

RESULTS

Figure (2a) illustrates typical pressure (bottom) and NO-absorption (top) oscilloscope traces at the fixed location 4.5 cm from the end wall, for a mixture of 26% nitromethane in argon. The first two numbers at the top of the figure refer to the oscilloscope gain (pressure, NO-absorption) while the third one refers to the time increment per division. The sudden jump in the NO absorption trace marks the arrival time of the reflected shock. At 70-80 μs, after the pressure jump caused by the reflected shock, there is another pressure jump that signals the end of the induction period. This coincides with the NO trace suddenly leveling off. Figures (2b-2d) illustrate typical pressure traces recorded at the end wall for pure nitromethane. The pressure jump in each record designates the reflected shock while the pressure spike indicates ignition. The latter is more pronounced for higher reflected shock pressures. The induction times are 25-30 μs, 10-12 μs, and 5 μs, respectively. The slow pressure rise following the reflected shock in Fig. 2c is due to the residual particle motion towards the end wall, typical when the reflected shock sweeps through a channel narrowed by the growth of the boundary layer on the side walls. The final products, H_2O, CO, CO_2, NO, NO_2, HCN, C_2H_4, C_2H_2, were consistently observed.

Measured induction times and those calculated by integrating the rate equations for an adiabatic constant volume process are listed in Table II for different initial conditions ranging from 1000 to 1600 K and 1 to 10 atm. Most of the data listed are for 100% nitromethane. The results for temperatures above 1600 K (behind the reflected shock) were disregarded because the incident shock is then strong enough to cause a significant decomposition of the starting material. Moreover, for temperatures above 1600 K the induction time is so short that it was impossible to distinguish between the reflected

the estimation of Arrhenius parameters for the isomerization of alkoxy radicals to hydroxyalkyl radicals, a structurally analogous change. We have assumed a strain energy of 26 kcal/mole for the 4-membered ring transition state in this case.

15. Baulch, D., Drysdale, D., Horne, D., and Lloyd, A., Evaluated Kinetic Data for High Temperature Reactions, Vol. I, The University of Leeds, 1972.

16. Baulch, D., Drysdale, D., Duxbury, J., and Grant, S., Evaluated Kinetic Data for High Temperature Reactions, Vol. III, The University of Leeds, 1976.

17. (a) Greiner, N. R., J. Chem. Phys., 53, 1070 (1970). This reference reports several measured H-abstraction rate constants for OH and derived expressions for OH reaction rates with primary, secondary, and tertiary R-H bonds. The following references, 17b - 17e, describe our use of this data.

(b) For CH_3NO and CH_3NO_2, a primary C-H bond energy was assumed, and A and E were calculated from Greiner's expression.

(c) Greiner's measurement of the rate constant for ethane was used.

(d) A secondary C-H bond strength was assumed for CH_3OH based upon reference 18's measurement of the C-H bond strength of methanol = 94 kcal/mole, and A and E were calculated from Greiner's expression.

(e) For the reaction, $OH + C_2H_4 \rightarrow C_2H_3 + H_2O$, we used 2/3 of the A factor for OH + ethane, and estimated the activation energy based upon the C-H bond energy of 109 kcal/mole reported by reference 22.

18. Golden, D. M., and Benson, S. W., Chem. Revs., 69, 125 (1969).

19. Baulch, D. L., Cox, R. A., Hampson, R. F., Kerr, J. A., Troe, J., and Watson, R. T., J. Phys. Chem. Ref. Data, 9, 295 (1980).

20. Atkinson, R., Darnall, K. R., Lloyd, A. C., Winer, A. M., and Pitts, J. N., Adv. Photochem., 11, 375 (1979).

21. Smith, I.W.M. and Zellner, R., J. Chem. Soc. Faraday Trans. II, 69, 1617 (1973).

22. (a) Benson, S. W., Thermochemical Kinetics, 2d ed, Wiley, N. Y., 1976.

(b) Trotman-Dickenson, A. F. and Steacie, E. W. R., J. Chem. Phys., 19, 329 (1951).

(c) It should be noted that the very old measurements of Ref. 22b yield an Arrhenius A factor in virtually exact agreement with one calculated by Benson (Ref. 22a, Table 4.6). The latter calculation is for $\Delta C_v(T)$ for the reaction. We used the same transition state model, but for ΔS_{act} we added 2R(ln2) to account for changes in symmetry and spin which are obviously necessary.

23. See Ref. 22b. For the reactions of CH_3 with CH_3NO_2 and CH_3NO we used 1/2 of A for $CH_3 + C_2H_6$ and the same E.

24. Hoyermann, K., Sievert, R., and Wagner, H. Gg., Ber. Bunsenges. Phys. Chem., 85, 149 (1981).

25. Westenberg A. A. and deHaas, N., J. Phys. Chem., 76, 2213 (1972).

26. Camilleri, P., Marshall, R. M., and Pernell, J. H., J. Chem. Soc. Faraday Trans. I, 70, 1434 (1974).

27. James, F. C. and Simons, J. P., Int. J. Chem. Kinet., 6, 887 (1974).

28. (a) Adams, G. F., Bartlett, R. J., and Purvis, G. D., Chem. Phys. Lett., 87, 311 (1982).

(b) Saebo, S., Radom, L., and Schaeffer III, H. F., J. Chem. Phys., 78, 845 (1983).

(c) From refs. 28a and b we have taken the lower E (= 39.5 Kcal/mole) of 28a, and have estimated $A = 10^{13}$ s^{-1} assuming a tight transition state.

29. Baldwin, R. R. and Melvin, A. J., J. Chem. Soc., 1785 (1964).

30. For the reactions of H with CH_3NO_2 and CH_3NO we have used the same E and 1/2 of A for the reaction H + C_2H_6, see ref. 29.

31. We note that the reactions H + C_2H_6 and CH_3 + C_2H_6 have a ratio of A factors of $A(H)/A(CH_3)$ = 400, and a difference in activation energies of $E(CH_3)$ - E(H) = 1100 cal/mole, based upon experimental measurements of refs. 22 and 29. Lacking experimental data we ahave assumed that the same relationships hold for reactions of H and CH_3 with all RH. Thus we estimated Arrhenius parameters for CH_3 + CH_3OH from ref. 24, and for CH_3 + CH_2O from ref. 25.

32. Stull, D. P., Westrum Jr., E. F., Sinke, G. C., The Chemical Thermodynamics of Organic Compounds, Wiley, N. Y., 1969.

33. Glanzer, K., Quack, M., and Troe, J., Sixteenth Symposium (International) on Combustion, The Combustion Institute, Pittsburgh, 1976, p. 949.

34. (a) Young, T. R. and Boris, J. P., J. Phys. Chem, 81, 2424 (1977).
(b) Young, T. R., NRL Memorandum Report 4091, Naval Research Laboratory, Code 4040, Washington, D. C., 20375-5000, 1980.

END

FILMED

9-85

DTIC